Climate Control on Net Primary Productivity in the Complicated Mountainous Area: A Case Study of Yunnan, China

Xiaobin Guan, Huanfeng Shen, *Senior Member, IEEE*, Xinghua Li, *Member, IEEE*, Wenxia Gan, and Liangpei Zhang, *Senior Member, IEEE*

***Abstract*—In this study, the influence of altitude on the relationship between vegetation and climate was investigated via net primary productivity (NPP) in the mountainous Yunnan province of China. In order to undertake a detailed spatial analysis at a long-term level, a monthly 1-km NPP time series from 1982 to 2014 was constructed from multisource remote sensing data sets. The altitudinal variation of the relationship between NPP and climatic factors was disclosed at annual, seasonal, and monthly scales, respectively. The results indicated that the correlation between NPP and precipitation gradually decreases from positive to negative with the ascending elevation at an annual scale, which is completely the opposite to temperature. The relationships at seasonal and monthly scales are also consistent, but significant seasonal heterogeneity was found due to the uneven climate. It was also concluded that downward run-off is responsible for the altitudinal heterogeneity, in that high-elevation areas cannot easily retain water, and only low-elevation areas benefit from the increased precipitation. What is more, we also found that the impact of climatic drought on NPP is related to topography. Large river valleys help to facilitate droughts, but the negative impacts on NPP can be mitigated in the rugged area with fluctuating slope.**

***Index Terms*—Climate control, drought, elevation transect, multisource remote sensing, net primary productivity (NPP).**

I. Introduction

NET primary productivity (NPP) is the biomass increment of plants in a specified time interval, which means that the residual amount of organic matter produced by vegetation photosynthesis was deducted from autotrophic respiration [1]–[3]. NPP is an important ecological indicator for the variation and balance of the terrestrial ecosystem carbon budgets. With the development of satellite technology, macroscopic and dynamic NPP can be modeled through remote sensing methods, and it has been comprehensively applied to the vegetation monitoring in recent years [4]–[6]. Under the background of drastic global climate change, the relationship between NPP and climate has become one of the most important core issues worldwide [7], [8]. Improved cognition of vegetation variation and adaptability to climate is essential to advance our understanding of global climate change and help the policies developing [9], [10].

Many studies have explored the relationship between the terrestrial ecosystem and climatic factors at regional, national, or global scales, and different conclusions about their spatial and temporal heterogeneity have been obtained [11]–[15]. Globally, Nemani *et al*. [12] suggested that global NPP increased by 6% from 1982 to 1999 due to climate change easing some of the critical climatic constraints to plant growth. At the hemisphere scale, Piao *et al*. [11] found that autumn warming has led to net carbon dioxide losses in northern terrestrial ecosystems, offsetting 90% of the increment during spring. Nationally, Liang *et al*. [13] indicated that the interannual variation of NPP is controlled by the air temperature throughout China, except for some arid and semiarid regions, where precipitation is the dominant factor. Regionally, Chen *et al*. [14] declared that the warm-wet climate increased the NPP of alpine grassland over the Qinghai–Tibet Plateau from 1982 to 2001, but the warm-dry climate decreased it in the last ten years. What is more, the impacts of extreme climate phenomena on NPP have also been intensively studied, including El Niño, heat, droughts, and so on [16]–[18]. With more and more frequent droughts occurring worldwide, a great deal of research has addressed the association between NPP anomalies and droughts in different regions [19]–[21].

However, almost all of the previous findings about the spatial differences of climate control on NPP are based on longitude, latitude, and vegetation types, but only a handful of studies that have paid attention to the altitudinal heterogeneity [22]–[25]. The data employed in most of the related studies were from the specific sites, and only the impacts of temperature were considered [26]–[30]. So they could only describe the performances of

Manuscript received September 15, 2017; revised June 14, 2018; accepted July 30, 2018. This research was supported by the National Natural Science Foundation of China (41271376, 41422108), and National Key R&D Program of China (2017YFA0604402). *(Corresponding author: Huanfeng Shen.)*

X. Guan is with the School of Resource and Environmental Sciences, Wuhan University, Wuhan 430072, China (e-mail: guanxb@whu.edu.cn).

H. Shen is with the School of Resource and Environmental Sciences, Wuhan University, Wuhan 430072, China, and also with the Collaborative Innovation Center for Geospatial Information Technology, Wuhan 430079, China (e-mail: shenhf@whu.edu.cn).

X. Li is with the School of Remote Sensing and Information Engineering, Wuhan University, Wuhan 430072, China (e-mail: lixinghua5540@whu.edu.cn).

W. Gan is with the School of Resource And Civil Engineering, Wuhan Institute of Technology, Wuhan 430073, China (e-mail: charlottegan@whu.edu.cn).

L. Zhang is with the State Key Laboratory of Information Engineering in Surveying, Mapping, and Remote Sensing, Wuhan University, Wuhan, 430072, China, and also with the Collaborative Innovation Center for Geospatial Information Technology, Wuhan 430079, China (e-mail: zlp62@whu.edu.cn).

Color versions of one or more of the figures in this paper are available online at http://ieeexplore.ieee.org.

Digital Object Identifier 10.1109/JSTARS.2018.2863957

the elevation points with sites distributed, no conclusion along the continuous elevation transect was obtained. In addition, the limited remote sensing research has only paid attention to the distribution of NPP with regard to elevation, slope, and aspect, but the analysis of its relationship to climate is lacking [22], [31]. Further study is also limited by the characteristics of the current satellite data sets, because none of them can provide both a suitable resolution and a long time span simultaneously [32]–[34]. In fact, it is also of great significance to explore the effect of climate on vegetation growth along elevation transects in complicated mountainous areas [35], [36]. Mountainous areas host approximately a quarter of the land surface and more than a third of the terrestrial plant species [35]. They also provide excellent natural laboratories for understanding the environmental controls on the ecosystem in various circumstances over short spatial distances [25]. Due to the complex natural conditions caused by the varied climatic factors, soil water movement, and the species change along elevation gradients [31], [37], the relationship between NPP and climate in mountainous areas is highly complicated. Therefore, cognition for the altitudinal heterogeneity of climate control on vegetation NPP is meaningful but currently lacking, and significant effort is urgently needed to acquire a better understanding.

Yunnan province is the most southwestern part of China, with more than 90% of the region covered by mountainous landforms. The elevation ranges from 76 to 6740 m, with very high vegetation coverage, so it is an ideal laboratory to study the heterogeneity of the relationship between NPP and climatic factors along altitudinal transects [25], [35]. What is more, the region is an important carbon sink [38], but has frequently suffered from droughts in recent decades [21], [39]. Although some studies have focused on the impacts of climatic factors and drought on NPP in this area, none of them have paid attention to the effect of elevation. Therefore, the main purpose of this paper is: 1) to obtain an appropriate long-term NPP time series with a suitable spatial resolution based on multisource remote sensing data sets and the multisensor information fusion method; 2) to undertake an in-depth investigation of the relationship between NPP and climatic factors along altitudinal gradients, as well as the seasonal heterogeneity; and 3) to explore as to whether or not there are effects of complicated topography on the relationship between NPP and drought in Yunnan.

II. Materials and Methods

A. Study Area

Yunnan province, located between 97.52°–106.18°E and 21.13°–29.25°N neighboring the Tibetan Plateau, is the most southwestern part of China [see Fig. 1(a)]. Mountainous landforms are the main terrain type, with highly varied elevation ranging from 67 to 6740 m only in the total area of 394 000 km^2. As shown in Fig. 1(b), a generally downward tendency in elevation from north to south can be observed. Vegetation covers approximately 94% of the area, and the complex mountainous landforms provide ideal conditions for the growth of rich vegetation types, varied from tropical species to frigid species [40]. The climate pattern is very diverse, with the synergistic effect

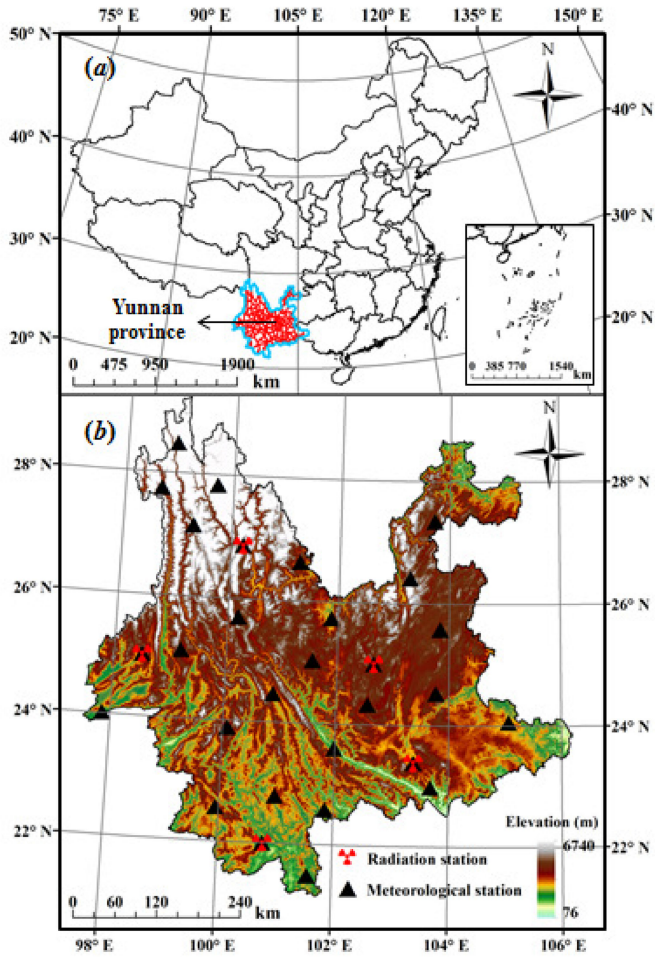

Fig. 1. Study area. (a) Location of Yunnan in China. (b) Spatial distribution of elevation in Yunnan province.

of different climate types, and the accordant decreasing impact on temperature by altitude and latitude from south to north aggravates the complexity. In addition, more and more frequent droughts have occurred in recent decades, and the area suffered from a continuous four-year extreme drought from 2009 to 2012 [21], [39]. Given that the importance of elevation in vegetation studies has been emphasized in previous research [25], [35], it is important to investigate the altitudinal heterogeneity of the climate control on NPP in Yunnan province, which is an important carbon sink with complex terrain and frequent droughts.

B. Data Sources

1) Remote Sensing Data: In this study, the advanced very high resolution radiometer global inventory modeling and mapping studies third generation (GIMMS3g) normalized difference vegetation index (NDVI) product and the moderate resolution imaging spectroradiometer (MODIS) MOD13A3 data collection were employed to composite a new NDVI time series, combining the respective advantages of time span and spatial resolution. The GIMMS product is the half-monthly NDVI at a spatial resolution of 8 km from 1982 to 2013, and the MOD13A3 product is 1-km data with a one-month time interval from 2000 to 2014. The two data sets are the most popular NDVI products

at the present time, and they have been widely applied in many studies [15], [22], [41].

The land-cover map was derived by the Environmental and Ecological Science Data Center for West China (WESTDC), and is named WESTDC2.0. The map integrates the information of the surveyed 1:100 000 land-resources data and multisource satellite land-cover data sets [42]. The vegetation types are synthesized into eight classes: evergreen broadleaf forest, deciduous broadleaf forest, needle-leaf forest, mixed forest, shrub, grass, crop, and other coverings. The applied digital elevation model (DEM) was the shuttle radar topography mission data set with a spatial resolution of 90 m, which was resampled to the scale of MODIS NDVI.

2) Meteorological Data: The meteorological data were from the China Meteorological Administration (CMA), comprising monthly precipitation, air temperature and daily surface pressure, air temperature, surface air relative humidity, and sunshine duration for 29 uniformly distributed stations, over the study period of 1982–2014. Observed solar radiation data from five radiation stations were also obtained. The ANUSPLIN package was employed to carefully interpolate the station records to the same spatial resolution as MODIS NDVI [43].

3) Field-Based NPP Data: The measurement-based biomass/NPP data set was derived from Luo's study [44], which has been extensively applied as validation data in many studies [45], [46]. The data for the study area were originally obtained by the Yunnan Ministry of Forestry. The data include the forest biomass/NPP and part values of various plant components, as well as the dominant species, latitude, longitude, and elevation of each site. However, the records of NPP are provided with the unit of dry matter (t.DM.ha^{-1}.year^{-1}), so a conversion factor of 50 was needed to change this into carbon content (gC.m^{-2}.year^{-1}) [46], [47].

4) Yearbook of Meteorological Disasters: The drought conditions of each district in Yunnan province were obtained from the Yearbook of Meteorological Disasters in China [48], which is the official published statistics. The yearbooks have declared the specific districts that have suffered from droughts every year, and the drought frequency of every district has been counted over the past ten years from 2004 to 2013.

C. NPP Estimation

1) Carnegie–Ames–Stanford Approach (CASA) Model: The CASA model was applied to estimate the monthly NPP in the study area. This model calculates NPP as the product of absorbed photosynthetic active radiation (APAR, MJ.m^{-2}) and the light-use efficiency (ε, gC.MJ^{-1}) [49]–[51], as follows:

$$\mathrm{NPP}\,(x,t) = \mathrm{APAR}\,(x,t) \times \varepsilon\,(x,t) \tag{1}$$

where $\mathrm{NPP}(x,t)$ is the total fixed NPP of pixel x in month t, $\mathrm{APAR}(x,t)$ is the total amount of absorbed photosynthetic active radiation over the period, and $\varepsilon(x,t)$ is the actual light-use efficiency. The calculation of APAR and ε is shown in (2) and (3), respectively:

$$\mathrm{APAR}\,(x,t) = R_s\,(x,t) \times 0.5 \times \mathrm{FPAR}\,(x,t) \tag{2}$$

$$\varepsilon\,(x,t) = \varepsilon^*(x,t) \times T(x,t) \times W(x,t) \tag{3}$$

where $R_s(x,t)$ is the total solar radiation, which was precisely calculated by the improved Yang hybrid model [52]–[54]; the coefficient 0.5 is the approximate ratio of photosynthetic active radiation (0.4–0.7 μm) in total solar radiation; and $\mathrm{FPAR}(x,t)$ is the fraction of photosynthetic active radiation absorbed by the vegetation canopy, which is a function of the NDVI. In (3), $\varepsilon^*(x,t)$ is the maximum light-use efficiency, which varies with the vegetation type according to the previous studies of ecosystems in China [55]; and $T(x,t)$ and $W(x,t)$ are the temperature stress factor and water stress factor [56], [57].

2) NDVI Construction: The spatial and temporal resolution of NPP from the CASA model was determined by the input NDVI, but a single remote sensing data set cannot provide a continuous long-term time series with a suitable spatial resolution. GIMMS3g spans a long period with a sparse resolution of 8 km, so it cannot provide enough spatial details and would lead to NPP accuracy loss [58], [59]. The MODIS product provides a suitable resolution range from 250 m to 1 km, but no data were observed before the year 2000. The spatial and temporal fusion model is an efficient way to combine the respective advantages of different remote sensing data sets and improve the data resolution with good accuracy [32], [60]–[62], and it has already been successfully applied to many vegetation studies to help conducting the analysis at a finer scale [33], [63], [64]. As a result, a multisource data fusion framework was constructed to obtain a monthly NDVI time series with a spatial resolution of 1 km from 1982 to 2014 [65]. First of all, the moving weighted harmonic analysis method was employed to correct the contaminated values caused by atmospheric contamination [66], and the pixel-by-pixel linear regressive model was used to narrow the sensor differences based on the mutually pairwise data [67]. Afterwards, the spatio-temporal information fusion method based on a nonlocal means filter was applied to improve the spatial resolution of the GIMMS3g data before 2000. Multisensor fusion can predict the fine-resolution (*F*) NDVI at t_k based on the coarse-resolution (*C*) data at t_k and the *F* and *C* acquired at t_0, expressed as

$$F(x_{w/2}, y_{w/2}, t_k) = \sum_{i=1}^{w}\sum_{j=1}^{w} W_{ij} \times F(x_i, y_j, t_0) + C(x_i, y_j, t_k) - C(x_i, y_j, t_0)) \tag{4}$$

where w is the size of the moving window; (x,y) denote the pixel location; and W_{ij} is the spatial weighting function, the more reasonable calculation of which is the applied fusion algorithm. The 1 km monthly NDVI data from 1982 to 1999 were fused referring to the pairwise data of corresponding month in the nearest year. The reliability of the NDVI construction processes was proved in our previous study, with root-mean-square error around 0.07 stably [68].

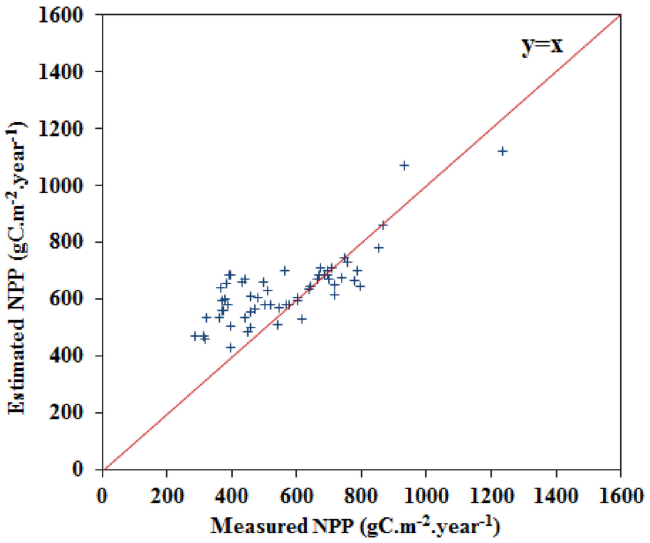

Fig. 2. Validation of the estimated NPP against field measurements ($r = 0.79$, $p < 0.001$, $N = 59$).

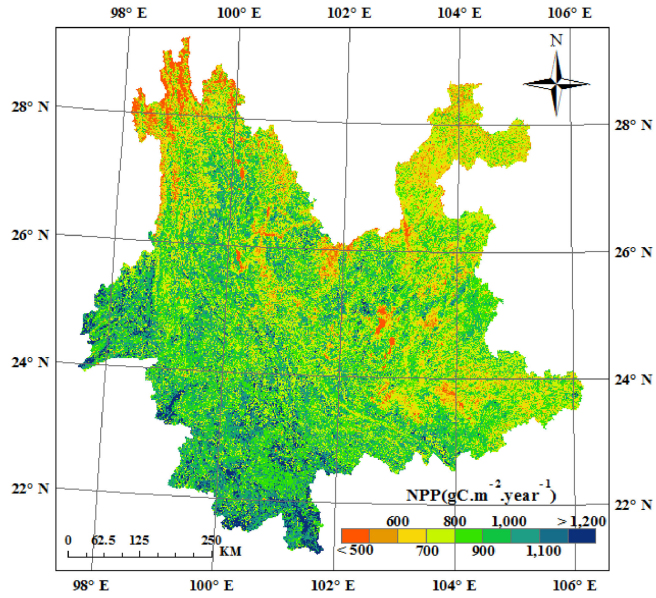

Fig. 3. Spatial distribution of NPP in Yunnan province.

D. Altitudinal Statistics

A simple equal division of elevation was employed to investigate the altitudinal heterogeneity of the relationship between NPP and climatic factors, which is an approach that has been commonly used in previous studies [22]. Synthetically considering the accuracy of the DEM data, the wide range of elevation, and the spatial resolution of the NPP time series, the step size of the elevation was set at 50 m [69]. According to previous research, permanent snow exists in the study area above the elevation of 4500 m [70]. Therefore, considering the vegetation coverage, only the region below the snow line was analyzed in this study, and totally 90 elevation segments were obtained. The Pearson correlation coefficient (r) was applied to represent the relationship between NPP and climatic factors.

III. Results and Analysis

In this section, the accuracy of the NPP time series was first validated before it was applied to analyze the altitudinal impacts on NPP distribution and variation. The heterogeneity of the relationship between NPP and climatic factors along the elevation transects was then explored at different time scales. Finally, the impact of elevation on the frequency of droughts in Yunnan was analyzed through the use of zonal statistics.

A. NPP Validation

In order to verify the reliability of the CASA model, the estimated NPP was validated against the field measurements of the Yunnan Ministry of Forestry from Luo's study [44]. In total, 59 records for the year 1983 were picked through matching the vegetation type with the land-cover map, and were then compared with the estimated NPP of the corresponding pixels. The verification result is shown as a scatterplot in Fig. 2, where the linear correlation coefficient between the estimated NPP and the field measurements reaches 0.79 ($p < 0.001$). This means that the estimated NPP by the CASA model can be deemed as reliable to study the carbon cycle in the study area.

B. NPP Variation Along Elevation Transect

In order to determine the altitudinal impact on NPP distribution and variation, the mean annual NPP for the different elevation zones was calculated and analyzed. Furthermore, the altitudinal difference of the NPP interannual variation is also visualized using a three-dimensional (3-D) diagram.

1) NPP Spatial Distribution: The spatial distribution of NPP in Yunnan province is shown in Fig. 3, where it can be seen that the overall tendency of NPP decreases from south to north, which is completely the opposite to the distribution of elevation shown in Fig. 1. This means that NPP is relatively low in the high mountain regions, and high NPP can be found in the low-elevation areas. To allow a detailed interpretation, the mean NPP for the different elevation zones with an isometric interval of 50 m was calculated. As shown in Fig. 4(a), it can be clearly observed that NPP decreases as the elevation increases, and the decreased trend (the slope) is greater and greater. The mean annual NPP is greater than 800 $gC.m^{-2}.year^{-1}$ in the low-elevation areas, but is less than 600 $gC.m^{-2}.year^{-1}$ when the elevation is higher than 4000 m. This is a result of the decrease in precipitation and temperature when the elevation becomes higher, as shown in Fig. 4(b). The abnormal trough in the NPP variation around the elevation of 1800 m conforms to the variation of precipitation. The precipitation reaches peak at the elevation around 1000 m and decreases in the higher area, which means the maximum precipitation height in the region. There is an abnormal U-sharped variation of NPP within the elevation of 0–600 m, where the vegetation is synergistic affected by the increased surface water and decreased temperature. Furthermore, statistical and representative error could also exist within this elevation range, because only a few pixels are covered, with a

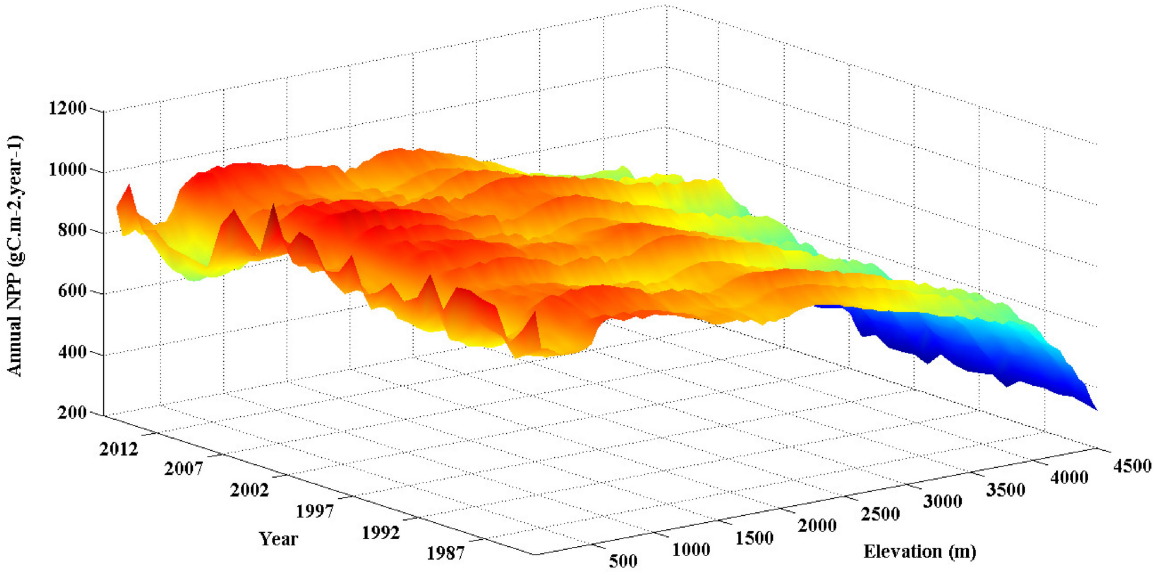

Fig. 4. Statistics of NPP and climatic factors in different elevations. (a) NPP. (b) Climatic factors.

total percentage of 1.25%. As shown in Fig. 4(a), 52.47% of Yunnan lies within the elevation range of 1500–2500 m, while the proportions with elevations higher than 3500 m and lower than 1000 m are very small. In general, the NPP overall decreases from the low-elevation grounds to the high-elevation mountains and agrees to both decline of precipitation and temperature.

2) NPP Annual Variation: The 3-D variation of NPP with regard to elevation and year is shown in Fig. 5. For the longitudinal profile of each year, the variation of NPP with elevation is very similar for the different years, except for the years from 2009 to 2012, when the area suffered persist severe drought. During these four years, the NPP of the low-elevation area does not show the U-sharped variation, but shows a continuously flat surface at a very low value. Furthermore, similar troughs are also found for all the other elevation zones in these four years. This indicates that NPP was seriously influenced by the severe four-year drought, which is much more apparent in the low-elevation area. Meanwhile, for the transverse profiles, which represent the interannual variation of NPP for the elevation zones, they are quite different with the increase of elevation. This indicates that the variation trends of NPP also show huge differences for different elevations.

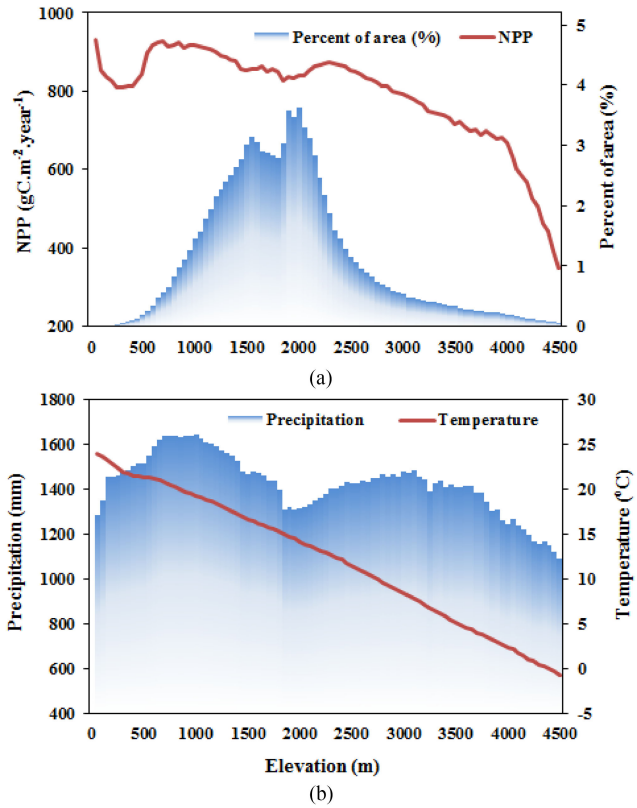

Fig. 5. Interannual variation of NPP in different elevations.

C. Quantitative Analysis of the Altitudinal Heterogeneity of Climate Control on NPP

In this section, quantitative correlation analysis is applied to explore the altitudinal variation of the relationship between NPP and climatic factors. The huge seasonal heterogeneity is carefully considered, and the issue is investigated at annual, seasonal, and monthly scales, respectively.

1) Annual Scale: The altitudinal variation of the climate control on NPP is first discussed at an annual scale. The Pearson correlation coefficient (r) between the annual NPP time series and climatic factors (i.e., annual mean temperature and annual cumulative precipitation) for the different elevation zones are shown in Fig. 6, where R_P and R_T denote the the Pearson correlation coefficient for precipitation and temperature, respectively. It can be clearly seen that the altitudinal variation of R_P is almost the opposite of R_T. Specifically, the correlation between NPP and precipitation shows a declining tendency as the elevation increases, from significantly positive to significantly negative. In contrast, the correlation between NPP and

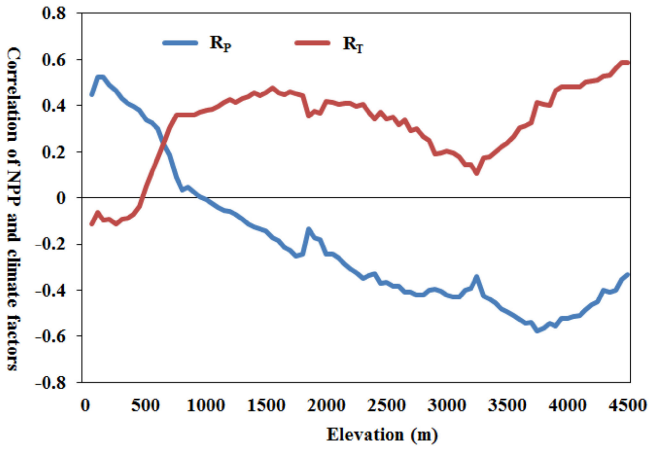

Fig. 6. Altitudinal variation of the correlation between annual NPP and climatic factors; R_P and R_T denote the correlation coefficients for precipitation and temperature, respectively.

temperature increases from the level of weakly negative to significantly positive. This is a result of the altitudinal distribution of precipitation and temperature, as well as the heterogeneous allocation of precipitation over the course of a year. In the low-elevation areas, temperature is appropriate for the photosynthesis of vegetation, but a warmer climate cannot always promote vegetation growth, and might have a negative effect on it. Thus, temperature shows a weak negative correlation with NPP. Meanwhile, temperature linearly decreases with the increase of elevation, and the negative impact is gradually replaced by a more and more strongly positive effect. An abnormal drop in the altitudinal variation of R_T occurs around the elevation of 3300 m, where there is the fog-prone area and the transition region with complex vegetation types. Fog prevents the transmission of solar radiation, which is the energy source of vegetation photosynthesis, and higher temperature can result in more fog. Thus, the positive correlation with NPP is weakened around the elevation.

According to our previous study [68], the significant negative correlation in the growing season (from May to October) dominates a weak annually negative correlation between NPP with precipitation in Yunnan province, due to the heterogeneous intraannual allocation of precipitation. In the growing season, there is abundant rainfall for vegetation photosynthesis, but the increased precipitation lessens the total solar radiation and instead suppresses vegetation growth. Moreover, the run-off of surface water flows from high-elevation areas to low-elevation areas, also resulting in the overall weak negative correlation between NPP and precipitation. Since most of the run-off gathers in the low-elevation areas, more precipitation increases the moisture in the low-elevation areas and further promotes the growth of vegetation. However, increased precipitation in the high-elevation areas can only add limited water, because of the water loss, but suppresses the vegetation growth as a result of the immediately reduced radiation. What is more, rain usually means lower temperature, which is the significant positive factor for vegetation in the high-elevation areas. As a result, the correlation between precipitation and NPP decreases along with increasing elevation, from positive to negative. Given that Yunnan province is mostly covered by lands around 2000 m, where precipitation is weakly correlated with NPP, the overall relationship of the region is also weakly negative. In conclusion, the correlation between NPP and precipitation decreases from positive to negative with ascending elevation, but the tendency is completely the opposite for temperature, which is a result of the uneven seasonal allocation of precipitation and the topographically downward run-off of surface water.

2) Seasonal Scale: Given that the uneven seasonal precipitation allocation has a huge impact on the relationship between climate and NPP, it is necessary to discuss these altitudinal variations at a seasonal scale. In order to examine the differences, the relationships are divided into four categories according to the the Pearson correlation coefficient (r) and P-value (p), respectively, are: significantly positive (SP, $r > 0$, $p < 0.05$); positive but not significant (NSP, $r > 0, p > 0.05$); significantly negative (SN, $r < 0$, $p < 0.05$); and negative but not significant (NSN, $r < 0$, $p > 0.05$). The percentage of area for each category in the different elevations in each season is shown in Fig. 7 (for R_P). For the relationship between seasonal NPP and precipitation, more areas show a positive relationship in the low-elevation region, and more areas show a negative relationship in the high-elevation region, for all the four seasons. In summer and autumn, positive correlation is the majority only in area with elevation lower than 600 m. Especially in summer, more than 90% of the area shows a negative correlation when elevation is higher than 1000 m, and more than half are the significant negative. Meanwhile, rare regions show a significant negative relationship in the spring and winter. Especially in winter, the positive relationship occupies the majority in the entire region with elevations lower than 2000 m. Furthermore, a high percentage of areas showing a positive correlation can be observed in all the elevation zones in spring. This is also a result of the uneven seasonal allocation of precipitation and the influence of topography. In summer and autumn, when precipitation is abundant, only the low-elevation areas can benefit from increased precipitation, because of the surface water run-off. At the same time, the high-elevation areas cannot retain the water from increased precipitation, and vegetation growth is suppressed by the reduced radiation and lower temperature. Meanwhile, in spring and winter, precipitation is much reduced and becomes the main limitation for vegetation growth in most of the areas. However, as temperature gradually turns into the main controlling factor for vegetation growth with the increase of elevation, so the positive impact of precipitation becomes much weaker and finally becomes negative, because more precipitation means lower temperature.

For the correlation between temperature and NPP, as shown in Fig. 8, areas with positive correlation are obviously the domination in all four seasons. Especially in winter, the area with significantly positive correlation occupies more than half of the area in most of the elevation zones. In summer, the large area showing negative correlation is due to the temperature being warm enough for vegetation growth, but significant negative correlation is also occasionally found. The weak negative

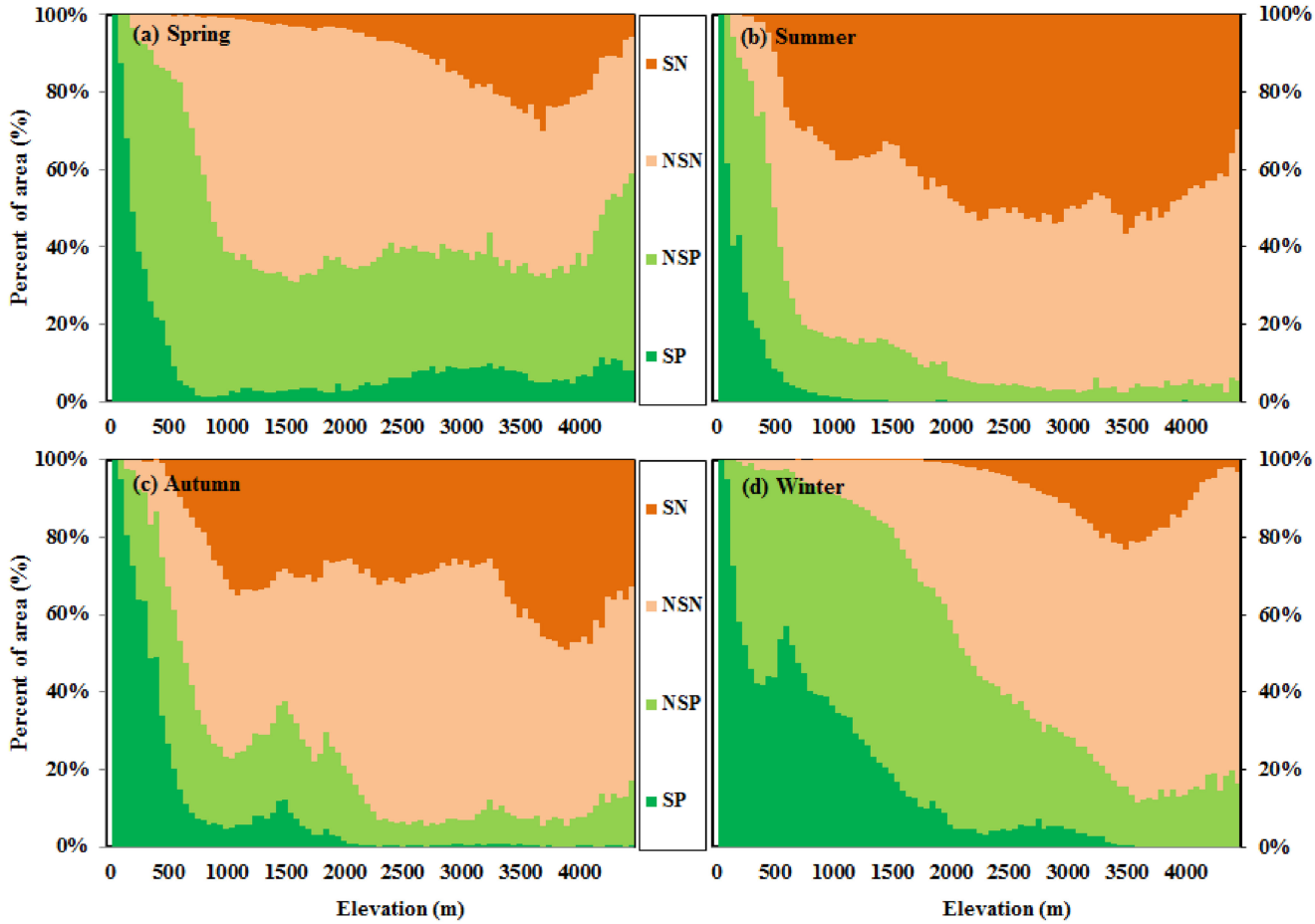

Fig. 7. Correlation between NPP and precipitation (R_P) for each season. (a) Spring. (b) Summer. (c) Autumn. (d) Winter. (SN: significantly negative; NSN: negative but not significant; NSP: positive but not significant; SP: significantly positive).

correlation in the low-elevation area at annual scale could also be the result of the correlation in summer. The abnormal drop in the relationship between NPP and temperature around 3300 m is also reflected in the figure, mostly in the seasons of autumn and winter. This phenomenon supports the reason given before, because the two seasons are the fog-prone period. Generally speaking, the correlation between NPP and precipitation shows a positive correlation in more areas in the low-elevation zones, and this phenomenon is maintained until much higher elevations in spring and winter. The positive correlation between NPP and temperature is almost the domination for all four seasons and all elevation area, except for some elevation zones in summer. This is consistent with the variation at an annual scale.

3) Monthly Scale: In order to further study the intraannual variation of the relationship between NPP and climatic factors, the R_P and R_T for each month were calculated along with the altitudinal gradient. As shown in Fig. 9, the variation of R_P by month and elevation shows a dustpan-shaped tendency. NPP shows a positive correlation with precipitation in almost all months in the low-elevation area, while completely the opposite relationship is found in the high-elevation area, with a totally negative correlation. Nevertheless, for the middle elevation zones, huge heterogeneity is observed for the different months. For the spring and winter months on the two sides, the continuously positive correlation is sustained until the elevation reaches 3000 m, and then gradually decreases into a negative relationship in the higher region. In contrast, for the summer months in the middle, the correlation becomes sharply negative after the elevation is higher than 500 m. This phenomenon could also be explained by the reason declared in the seasonal section, and further supports the fact that topography has an apparent impact on the climate control of NPP. Because of the downwards run-off of surface water, the water from rainfall cannot be easily retained in the high-elevation areas, and only vegetation in the low-elevation areas benefits more from it. As a result, in the summer months when precipitation is abundant, only the very low elevation region is positively correlated with precipitation, and the correlation immediately becomes negative in the higher areas. When precipitation is much reduced in the winter months and is insufficient for vegetation growth, the positive correlation lasts in the areas with very high elevation, until the replacement of temperature being the main limitation. In summary, the altitudinal heterogeneity of precipitation control on NPP is even more obvious at the monthly scale, with the positive correlation sharply turning into a negative correlation in the summer months, but persistently maintained until high elevations in the winter months. However, the altitudinal variation for the

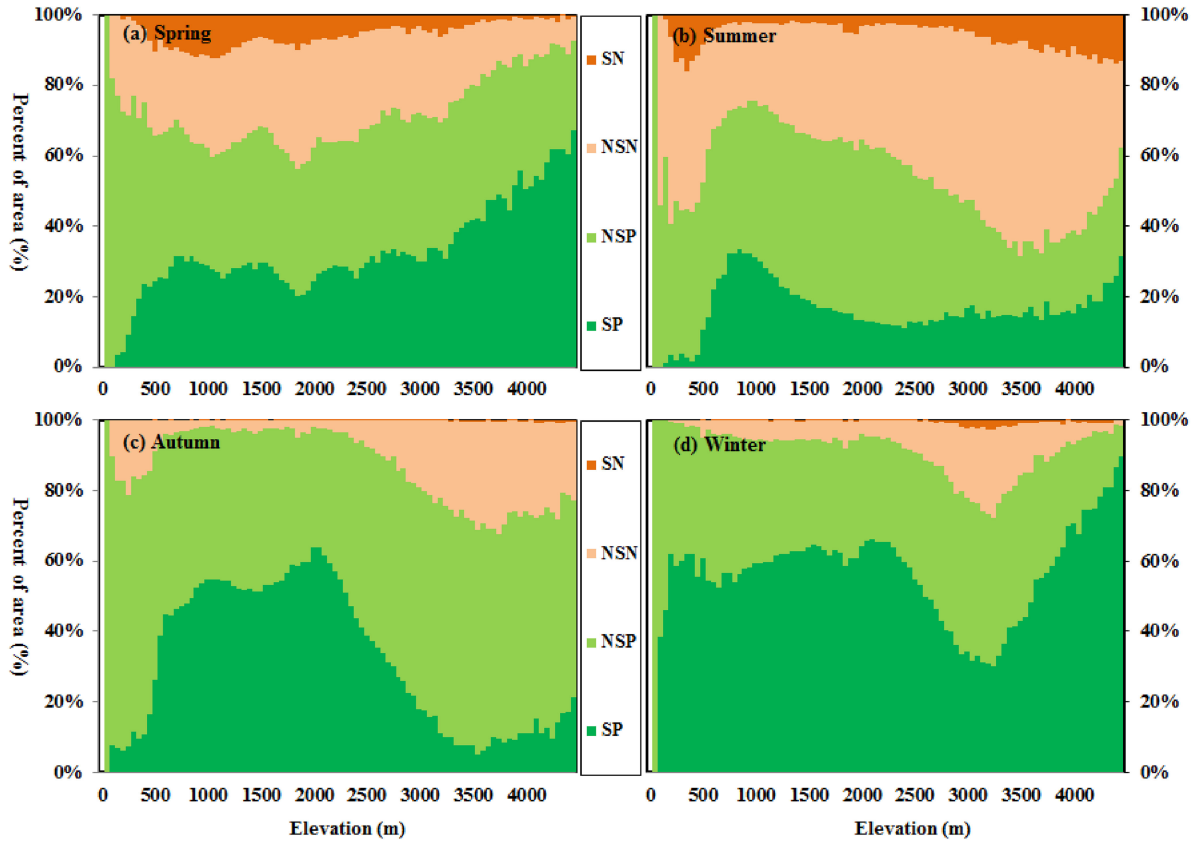

Fig. 8. Correlation between NPP and temperature (R_T) for each season. (a) Spring. (b) Summer. (c) Autumn. (d) Winter. (SN: significantly negative; NSN: negative but not significant; NSP: positive but not significant; SP: significantly positive).

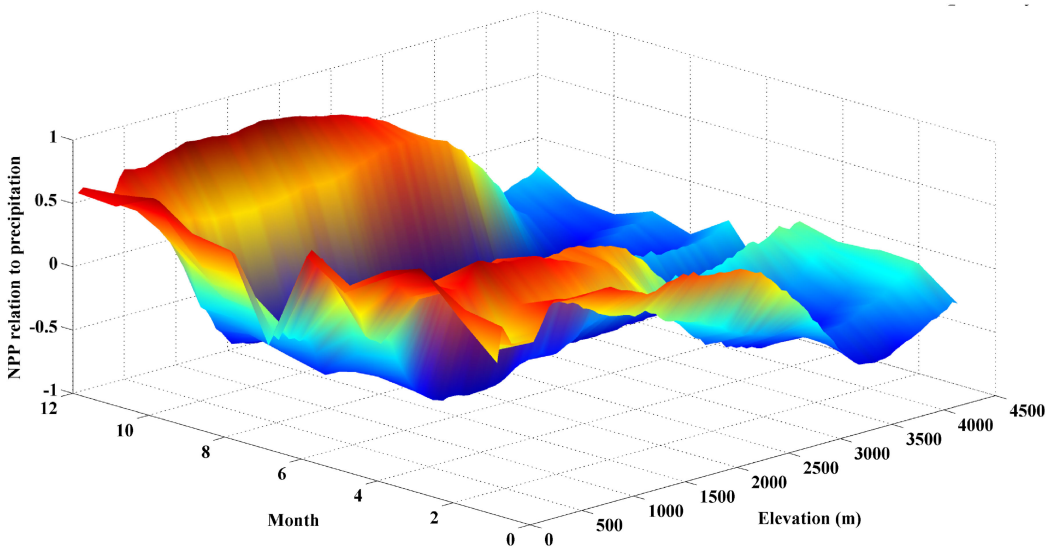

Fig. 9. Altitudinal variation of the relationship between monthly NPP and precipitation.

relationship between NPP and temperature is much messier, and needs further analysis.

D. Topographic Heterogeneity of the Drought Effect on NPP

Droughts have had severe impacts on the NPP in Yunnan [21]. Although the drought effect was usually supposed to vary with drought severity and vegetation types [71], [72], the regional topography should also be the factor because topographic water loss usually leads to droughts. So it is reasonable and necessary to discuss the topographic impacts on NPP from the aspect of climatic droughts. The drought frequency in the past ten years for each district was counted according to the disasters yearbook. Furthermore, a variety of factors was also calculated, including

TABLE I
STATISTICS OF THE DROUGHT FREQUENCY AND POTENTIAL FACTORS FOR EACH DISTRICT IN THE PAST DECADE

District	Drought frequency	Elevation (m)	Slope (°)	NPP ($gC.m^{-2}.year^{-1}$)	NPP_diff	P_mean (mm)	T_mean (°C)
Yuxi	7	1669.93	7.99	853.62	6.71	1366.80	16.70
Kunming	7	2050.98	6.68	807.47	18.73	1189.25	12.67
Lincang	6	1611.90	9.72	923.53	-6.68	1700.09	14.94
Honghe	6	1479.80	8.35	840.65	40.11	1452.39	16.28
Zhaotong	6	1607.07	9.87	686.02	40.04	1163.43	5.69
Baoshan	5	1807.31	8.78	927.44	7.39	1667.00	13.82
Wenshan	5	1332.33	5.40	778.01	70.13	1352.26	13.82
Lijiang	5	2557.07	11.20	798.33	5.40	1312.41	9.44
Qujing	5	2010.95	5.13	785.82	20.35	1157.95	11.15
Dali	4	2246.12	9.06	862.66	17.81	1434.42	13.44
Chuxiong	4	1915.21	7.94	829.32	−6.24	1276.09	14.80
Simao	3	1415.64	8.51	968.09	−19.34	1692.31	16.80
Diqing	2	3414.03	14.31	681.99	35.70	1283.13	0.96
Nujiang	0	2669.42	16.14	717.70	/	1792.67	0.63
Xishuangbanna	0	1059.17	6.63	1043.73	/	1771.74	15.91
Dehong	0	1357.11	7.67	1001.20	/	1755.24	11.64

Notes: P_mean and T_mean denote the mean precipitation and temperature in the past 10 years; NPP_diff is the difference between the NPP in drought years and non-drought years; a negative value means that the drought reduced the NPP, and a positive value means that the NPP increased in drought years.

the mean elevation, slope, temperature (T_mean), annual precipitation (P_mean), annual NPP in the past ten years, and the NPP difference (NPP_diff) between drought years and nondrought years. The results are shown in Table I, in descending order of drought frequency. In some districts that have suffered from frequent droughts, i.e., Lincang, Honghe, and Yuxi, the precipitation is abundant with high NPP. This indicates that precipitation is not the only determinant for droughts. From the overlay of the drought frequency and low-elevation areas in Fig. 10, it can be seen that large river valleys run through the three districts. These huge river valleys help to facilitate the frequent regional droughts, because the surface water flows down from the higher ground into the valleys. Therefore, droughts prefer to take place in the high-elevation areas when the precipitation declines.

The downward surface water loss causes the apparent altitudinal heterogeneity of the relationship between NPP and climate. Therefore, topography not only impacts the drought frequency, but also affects the NPP changes caused by droughts. The indicator of NPP_diff is used to evaluate the drought impact on NPP, and is defined as the difference in the NPP between drought and nondrought years. A negative NPP_diff means that drought reduced the NPP in the district, and a positive value means that NPP is increased. From Table I, it can be observed that the droughts in most areas have reduced the NPP in the past ten years, except for Simao, Lincang, and Chuxiong. The flat regions such as Wenshan, Qujing, and Kunming generally show high NPP_diff, which means that regional NPP has been dramatically reduced by droughts. Comparing the hierarchical graph of NPP_diff in Fig. 10 and the slope distribution in Fig. 11, an obvious consistency can be found between them. In east Yunnan,

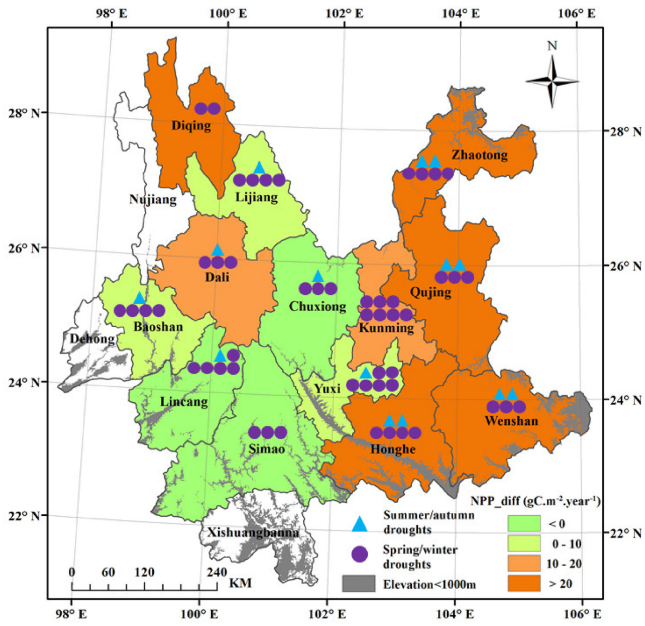

Fig. 10. Drought frequency and its impact on NPP for each district in Yunnan province. NPP_diff denotes the difference between the mean NPP in years without drought and in drought years, where a positive value means that the droughts decreased NPP. The blank blocks in Xishuangbanna, Dehong, and Nujiang mean that no droughts occurred.

where the terrain is extraordinary flat with entirely low slope, droughts have greatly reduced the NPP in all districts, with values larger than 20 $gC.m^{-2}.year^{-1}$. Nevertheless, for the districts where droughts have slightly reduced NPP or even increased it,

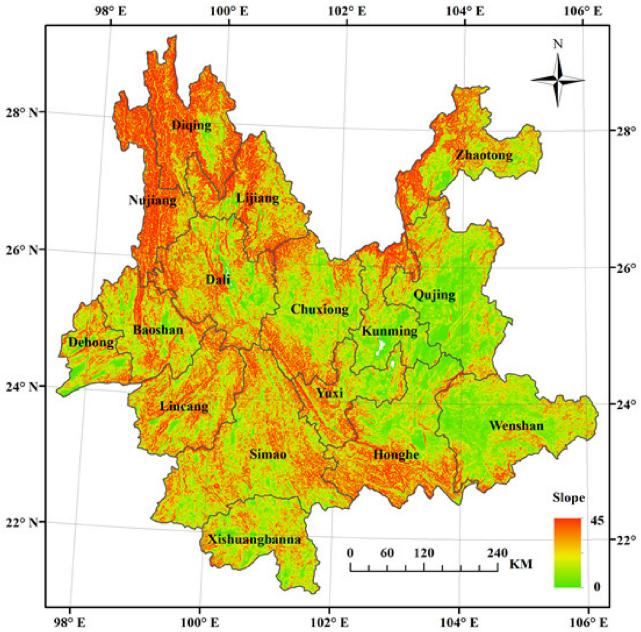

Fig. 11. Distribution of slope in Yunnan province.

the terrain is usually very rugged and fragmentized, especially for Simao and Lincang, where both mountainous and flat land is interspersed.

The reason for the impact of drought on NPP being related to topography could also be the result of the downward run-off of surface water. In the previous section, it was noted that the water flow from high mountains to low ground greatly enhances the possibilities of drought taking place in high-elevation areas. Therefore, in many droughts, although there is obvious water shortage in the high-elevation areas, water sources can also be abundant in the low-elevation areas. Under such circumstances, the NPP in the low-elevation areas does not decrease a lot, and may even increase due to the sufficient water and the much warmer climate during a drought period. For the high-elevation areas, the water shortage may not impact the vegetation growth as it would in other areas, because of the fine drought tolerance of the plants. Due to the perennially harsh environments in high-elevation areas with less water, the vegetation adapts to such conditions. Thus, in a region with complicated and fragmentized topography, drought may not evidently decrease the NPP, in both the low-elevation and high-elevation areas. Typically, as in Simao and Lincang, where mountains and flat land are interspersed, the droughts have had little impact on vegetation growth. However, for an area with overall flat topography, drought means that there is a severe water shortage in the whole region, so the drought enormously impacted NPP.

IV. Conclusion

In this paper, the heterogeneity of the relationship between NPP and climatic factors along altitudinal gradients was in-depth studied at a long-term level, in the mountainous Yunnan province of China. In order to provide more detailed spatial information, multisource remote sensing data were applied to obtain a 1-km NPP time series from 1982 to 2014. Analysis indicated that the climate control on NPP showed obvious altitudinal differences, either from the aspect of correlation or from the aspect of drought. It was found that the correlation between NPP and climatic factors evidently changed along elevation transect, and which greatly varied in different seasons. With the elevation increasing, the R_P continuously changed from significantly positive to significantly negative, but the R_T was completely the opposite. While, the seasonal heterogeneity showed that the positive R_P majority maintained until much higher elevations in spring and winter, when water was the main limitation for vegetation growth. The downward run-off of surface water should be responsible for the altitudinal heterogeneity, which resulted in that high-elevation areas cannot hold water, and only the low-elevation regions benefited from the precipitation. What is more, from the aspect of the drought impacts on NPP, we also found that the topography have certain effects on either the drought frequency or its impacts on NPP. On the one hand, the large river valleys facilitated the frequent droughts. On the other hand, the rugged topography with fluctuating slope helped lessening the negative influence of drought on NPP.

Since research into the heterogeneity of climate control on vegetation along altitudinal transects is lacking, this study concentrated on this topic and obtained interesting conclusions, which will be beneficial for the systematic understanding of global climate change. However, only the altitudinal impact was taken into consideration, and other topographic factors should be considered in further study, such as slope, aspect, vegetation species, and so on. Furthermore, the impact of elevation on frequent droughts should be further investigated quantitatively, using drought indexes with a suitable resolution.

Acknowledgment

The authors would like to thank the CMA and the NASA Ames Ecological Forecasting Lab and Earth Observing System for providing the necessary data sets. Special thanks are given to all the people who have provided helpful comments and suggestions.

References

[1] S. Piao, J. Fang, L. Zhou, B. Zhu, K. Tan, and S. Tao, "Changes in vegetation net primary productivity from 1982 to 1999 in China," *Global Biogeochem. Cycles*, vol. 19, pp. 1–16, 2005.

[2] R. Crabtree *et al.*, "A modeling and spatio-temporal analysis framework for monitoring environmental change using NPP as an ecosystem indicator," *Remote Sens. Environ.*, vol. 113, pp. 1486–1496, 2009.

[3] C. B. Field, J. T. Randerson, and C. M. Malmström, "Global net primary production: Combining ecology and remote sensing," *Remote Sens. Environ.*, vol. 51, pp. 74–88, 1995.

[4] M. Rees, R. Condit, M. Crawley, S. Pacala, and D. Tilman, "Long-term studies of vegetation dynamics," *Science*, vol. 293, pp. 650–655, 2001.

[5] W. Cramer *et al.*, "Comparing global models of terrestrial net primary productivity (NPP): Overview and key results," *Global Change Biol.*, vol. 5, pp. 1–15, 1999.

[6] C. Eisfelder, C. Kuenzer, S. Dech, and M. F. Buchroithner, "Comparison of two remote sensing based models for regional net primary productivity estimation—A case study in semi-arid central kazakhstan," *IEEE J. Sel. Topics Appl. Earth Observ. Remote Sens.*, vol. 6, no. 4, pp. 1843–1856, Aug. 2013.

[7] J. M. Melillo, A. D. McGuire, D. W. Kicklighter, B. Moore, C. J. Vorosmarty, and A. L. Schloss, "Global climate change and terrestrial net primary production," *Nature*, vol. 363, pp. 234–240, 1993.

[8] S. Piao *et al.*, "The carbon balance of terrestrial ecosystems in China," *Nature*, vol. 458, pp. 1009–1014, 2009.

[9] W. M. Post, T.-H. Peng, W. R. Emanuel, A. W. King, V. H. Dale, and D. L. DeAngelis, "The global carbon cycle," *Am. Sci.*, vol. 78, pp. 310–326, 1990.

[10] A. W. Seddon, M. Macias-Fauria, P. R. Long, D. Benz, and K. J. Willis, "Sensitivity of global terrestrial ecosystems to climate variability," *Nature*, vol. 531, pp. 229–232, 2016.

[11] S. Piao *et al.*, "Net carbon dioxide losses of northern ecosystems in response to autumn warming," *Nature*, vol. 451, pp. 49–52, 2008.

[12] R. R. Nemani *et al.*, "Climate-driven increases in global terrestrial net primary production from 1982 to 1999," *Science*, vol. 300, pp. 1560–1563, 2003.

[13] W. Liang *et al.*, "Analysis of spatial and temporal patterns of net primary production and their climate controls in China from 1982 to 2010," *Agricultural Forest Meteorology*, vol. 204, pp. 22–36, 2015.

[14] B. Chen *et al.*, "The impact of climate change and anthropogenic activities on alpine grassland over the Qinghai-Tibet Plateau," *Agricultural Forest Meteorology*, vols. 189–190, pp. 11–18, 2014.

[15] Y. Zhou, B. Xing, and W. Ju, "Assessing the impact of urban sprawl on net primary productivity of terrestrial ecosystems using a process-based model—A case study in Nanjing, China," *IEEE J. Sel. Topics Appl. Earth Observ. Remote Sens.*, vol. 8, no. 5, pp. 2318–2331, May 2015.

[16] G. P. Asner, A. R. Townsend, and B. H. Braswell, "Satellite observation of El Niño effects on Amazon Forest phenology and productivity," *Geophys. Res. Lett.*, vol. 27, pp. 981–984, 2000.

[17] P. Ciais *et al.*, "Europe-wide reduction in primary productivity caused by the heat and drought in 2003," *Nature*, vol. 437, pp. 529–533, 2005.

[18] M. K. van der Molen *et al.*, "Drought and ecosystem carbon cycling," *Agricultural Forest Meteorology*, vol. 151, pp. 765–773, 2011.

[19] M. Zhao and S. W. Running, "Drought-induced reduction in global terrestrial net primary production from 2000 through 2009," *Science*, vol. 329, pp. 940–943, 2010.

[20] D. Peng *et al.*, "Country-level net primary production distribution and response to drought and land cover change," *Sci. Total Environ.*, vol. 574, pp. 65–77, 2017.

[21] L. Zhang, J. Xiao, J. Li, K. Wang, L. Lei, and H. Guo, "The 2010 spring drought reduced primary productivity in southwestern China," *Environmental Res. Lett.*, vol. 7, pp. 1–10, 2012.

[22] Q. Gao *et al.*, "Effects of topography and human activity on the net primary productivity (NPP) of alpine grassland in northern Tibet from 1981 to 2004," *Int. J. Remote Sens.*, vol. 34, pp. 2057–2069, 2013.

[23] C. C. Cleveland *et al.*, "Relationships among net primary productivity, nutrients and climate in tropical rain forest: a pan-tropical analysis," *Ecology Lett.*, vol. 14, pp. 939–947, 2011.

[24] Z. Wang, T. Luo, R. Li, Y. Tang, and M. Du, "Causes for the unimodal pattern of biomass and productivity in alpine grasslands along a large altitudinal gradient in semi-arid regions," *J. Vegetation Sci.*, vol. 24, pp. 189–201, 2013.

[25] Y. Malhi, M. Silman, N. Salinas, M. Bush, P. Meir, and S. Saatchi, "Introduction: Elevation gradients in the tropics: Laboratories for ecosystem ecology and global change research," *Global Change Biol.*, vol. 16, pp. 3171–3175, 2010.

[26] B. Zhu *et al.*, "Altitudinal changes in carbon storage of temperate forests on Mt Changbai, Northeast China," *J. Plant Res.*, vol. 123, pp. 439–452, 2010.

[27] U. Shankar, H. N. Pandey, and R. S. Tripathi, "Phytomass dynamics and primary productivity in humid grasslands along altitudinal and rainfall gradients," *Acta Oecologica*, vol. 14, pp. 197–209, 1993.

[28] J. W. Raich, A. E. Russell, and P. M. Vitousek, "Primary productivity and ecosystem development along an elevational gradient on Mauna Loa, Hawai'i," *Ecology*, vol. 78, pp. 707–721, 1997.

[29] C. Leuschner, G. Moser, C. Bertsch, M. Röderstein, and D. Hertel, "Large altitudinal increase in tree root/shoot ratio in tropical mountain forests of Ecuador," *Basic Appl. Ecology*, vol. 8, pp. 219–230, 2007.

[30] C. A. J. Girardin *et al.*, "Net primary productivity allocation and cycling of carbon along a tropical forest elevational transect in the Peruvian Andes," *Global Change Biol.*, vol. 16, pp. 3176–3192, 2010.

[31] X. F. Chen, J. M. Chen, S. Q. An, and W. M. Ju, "Effects of topography on simulated net primary productivity at landscape scale," *J. Environmental Manage.*, vol. 85, pp. 585–596, 2007.

[32] F. Gao, J. Masek, M. Schwaller, and F. Hall, "On the blending of the Landsat and MODIS surface reflectance: Predicting daily Landsat surface reflectance," *IEEE Trans. Geosci. Remote Sens.*, vol. 44, no. 8, pp. 2207–2218, Aug. 2006.

[33] Q. Cheng, H. Liu, H. Shen, P. Wu, and L. Zhang, "A spatial and temporal non-local filter based data fusion method," *IEEE Trans. Geosci. Remote Sens.*, vol. 55, no. 8, pp. 4476–4488, Aug. 2016.

[34] H. Zhang, J. M. Chen, B. Huang, H. Song, and Y. Li, "Reconstructing seasonal variation of landsat vegetation index related to leaf area index by fusing with MODIS data," *IEEE J. Sel. Topics Appl. Earth Observ. Remote Sens.*, vol. 7, no. 3, pp. 950–960, Mar. 2014.

[35] C. Körner, "The use of 'altitude' in ecological research," *Trends Ecology Evol.*, vol. 22, pp. 569–574, 2007.

[36] M. K. Sundqvist, N. J. Sanders, and D. A. Wardle, "Community and ecosystem responses to elevational gradients: Processes, mechanisms, and insights for global change," *Annu. Rev. Ecol. Evol. Syst.*, vol. 44, pp. 261–280, 2013.

[37] M. S. Wigmosta, L. W. Vail, and D. P. Lettenmaier, "A distributed hydrology-vegetation model for complex terrain," *Water Resources Res.*, vol. 30, pp. 1665–1679, 1994.

[38] J. Fang, A. Chen, C. Peng, S. Zhao, and L. Ci, "Changes in forest biomass carbon storage in China between 1949 and 1998," *Science*, vol. 292, pp. 2320–2322, 2001.

[39] W. Yu, M. Shao, M. Ren, H. Zhou, Z. Jiang, and D. Li, "Analysis on spatial and temporal characteristics drought of Yunnan Province," *Acta Ecologica Sinica*, vol. 33, pp. 317–324, 2013.

[40] X. Li and D. Walker, "The plant geography of yunnan province, southwest china," *J. Biogeography*, vol. 13, pp. 367–397, 1986.

[41] L. Wang, W. Gong, Y. Ma, and M. Zhang, "Modeling regional vegetation NPP variations and their relationships with climatic parameters in Wuhan, China," *Earth Interactions*, vol. 17, pp. 1–20, 2013.

[42] Y. Ran, X. Li, and L. Lu, "China land cover classification at 1 km spatial resolution based on a multi-source data fusion approach," *Adv. Earth Sci.*, vol. 24, pp. 192–203, 2009.

[43] M. F. Hutchinson and T. Xu, *ANUSPLIN version 4.4 User Guide*. Canberra, Australia: The Australian Nat. Univ., 2013.

[44] T. Luo, "Patterns of net primary productivity for Chinese major forest types and their mathematical models," *Ph.D. dissertation, Chinese Acad. Sci.*, Beijing, China, 1996.

[45] F. Pei, X. Li, X. Liu, S. Wang, and Z. He, "Assessing the differences in net primary productivity between pre-and post-urban land development in China," *Agricultural Forest Meteorology*, vol. 171, pp. 174–186, 2013.

[46] J. Ni, "Net primary productivity in forests of China: scaling-up of national inventory data and comparison with model predictions," *Forest Ecology Manage.*, vol. 176, pp. 485–495, 2003.

[47] R. Myneni *et al.*, "A large carbon sink in the woody biomass of northern forests," *Proc. Nat. Acad. Sci.*, vol. 98, pp. 14784–14789, 2001.

[48] L. Song, *The Yearbook of Meteorological Disasters in China*. Beijing, China: Meteorological Press, pp. 2004–2013.

[49] C. S. Potter *et al.*, "Terrestrial ecosystem production: a process model based on global satellite and surface data," *Global Biogeochem. Cycles*, vol. 7, pp. 811–841, 1993.

[50] J. Monteith, "Solar radiation and productivity in tropical ecosystems," *J. Appl. Ecology*, vol. 9, pp. 747–766, 1972.

[51] C. Potter *et al.*, "Terrestrial ecosystem production: A process model based on global satellite and surface data," *Global Biogeochem. Cycles*, vol. 7, pp. 811–841, 1993.

[52] K. Yang, T. Koike, and B. Ye, "Improving estimation of hourly, daily, and monthly solar radiation by importing global data sets," *Agricultural Forest Meteorology*, vol. 137, pp. 43–55, 2006.

[53] K. Yang, G. W. Huang, and N. Tamai, "A hybrid model for estimating global solar radiation," *Solar Energy*, vol. 70, pp. 13–22, 2001.

[54] L. Wang, G. A. Salazar, W. Gong, S. Peng, L. Zou, and A. Lin, "An improved method for estimating the Ångström turbidity coefficient b in Central China during 1961e2010," *Energy*, vol. 30, pp. 67–73, 2014.

[55] W. Zhu, Y. Pan, and J. Zhang, "Estimation of net primary productivity of Chinese terrestrial vegetation based on remote sensing," *J. Plant Ecology*, vol. 31, pp. 413–424, 2007.

[56] G. Zhou and X. Zhang, "A natural vegetation NPP model," *Acta Phytoecologica Sinica*, vol. 19, pp. 193–200, 1995.

[57] G. Zhou and X. Zhang, "Study on npp of natural vegetation in China under global climate change," *Acta Phytoecologica Sinica*, vol. 1, pp. 11–19, 1996.

[58] D. P. Turner, R. Dodson, and D. Marks, "Comparison of alternative spatial resolutions in the application of a spatially distributed biogeochemical model over complex terrain," *Ecological Model.*, vol. 90, pp. 53–67, 1996.
[59] J. M. Chen, "Spatial scaling of a remotely sensed surface parameter by contexture," *Remote Sens. Environ.*, vol. 69, pp. 30–42, 1999.
[60] H. Shen, L. Huang, L. Zhang, P. Wu, and C. Zeng, "Long-term and fine-scale satellite monitoring of the urban heat island effect by the fusion of multi-temporal and multi-sensor remote sensed data: A 26-year case study of the city of Wuhan in China," *Remote Sens. Environ.*, vol. 172, pp. 109–125, 2016.
[61] S. Liu, W. Zhao, H. Shen, and L. Zhang, "Regional-scale winter wheat phenology monitoring using multisensor spatio-temporal fusion in a South Central China growing area," *J. Appl. Remote Sens.*, vol. 10, pp. 046029–046045, 2016.
[62] A. Ghulam, "Monitoring tropical forest degradation in betampona nature reserve, madagascar using multisource remote sensing data fusion," *IEEE J. Sel. Topics Appl. Earth Observ. Remote Sens.*, vol. 7, no. 12, pp. 4960–4971, Dec. 2014.
[63] H. Shen, X. Meng, and L. Zhang, "An integrated framework for the spatio–temporal–spectral fusion of remote sensing images," *IEEE Trans. Geosci. Remote Sens.*, vol. 54, no. 12, pp. 7135–7148, Dec. 2016.
[64] C. Han, H. Zhang, C. Gao, C. Jiang, N. Sang, and L. Zhang, "A remote sensing image fusion method based on the analysis sparse model," *IEEE J. Sel. Topics Appl. Earth Observ. Remote Sens.*, vol. 9, no. 1, pp. 439–453, Jan. 2016.
[65] H. Liu, P. Wu, H. Shen, and Q. Yuan, "A spatio-temporal information fusion method based on Non –Local Means Filter," *Geography Geo–Inf. Sci.*, vol. 31, pp. 27–32, 2015.
[66] G. Yang, H. Shen, L. Zhang, Z. He, and X. Li, "A moving weighted harmonic analysis method for reconstructing high-quality SPOT VEGETATION NDVI time-series data," *IEEE Trans. Geosci. Remote Sens.*, vol. 53, no. 11, pp. 6008–6021, Nov. 2015.
[67] W. Gan, H. Shen, L. Zhang, and W. Gong, "Normalization of medium-resolution NDVI by the use of coarser reference data: Method and evaluation," *Int. J. Remote Sens.*, vol. 35, pp. 7400–7429, 2014.
[68] X. Guan *et al.*, "A 33-year NPP monitoring study in southwest China by the fusion of multi-source remote sensing and station data," *Remote Sens.*, vol. 9, pp. 1082–1104, 2017.
[69] E. Rodriguez, C. S. Morris, and J. E. Belz, "A global assessment of the SRTM performance," *Photogrammetric Eng. Remote Sens.*, vol. 72, pp. 249–260, 2006.
[70] H. V. Wissmann, "The pleistocene glaciation in china," *Acta Geologica Sinica*, vol. 17, pp. 145–168, 1937.
[71] S. Chakrabarti, T. Bongiovanni, J. Judge, L. Zotarelli, and C. Bayer, "Assimilation of SMOS soil moisture for quantifying drought impacts on crop yield in agricultural regions," *IEEE J. Sel. Topics Appl. Earth Observ. Remote Sens.*, vol. 7, no. 9, pp. 3867–3879, Sep. 2017.
[72] Z. Gao, N. Xu, C. Fu, and J. Ning, "Evaluating drought monitoring methods using remote sensing: A dynamic correlation analysis between heat fluxes and land cover patterns," *IEEE J. Sel. Topics Appl. Earth Observ. Remote Sens.*, vol. 8, no. 1, pp. 298–303, Jan. 2015.

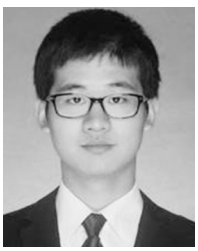

Xiaobin Guan received the B.S. and the Ph.D. degrees in geographical information system from the School of Resource and Environmental Sciences, Wuhan University, Wuhan, China, in 2013 and 2018, respectively.

His research interests include the processes of multisource remote-sensing images and their application in vegetation monitoring, and the interactive relationship between the global change and terrestrial ecosystem.

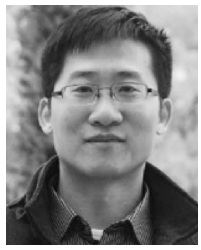

Huanfeng Shen (M'11–SM'13) received the B.S. degree in surveying and mapping engineering and the Ph.D. degree in photogrammetry and remote sensing from Wuhan University, Wuhan, China, in 2002 and 2007, respectively.

In July 2007, he joined the School of Resource and Environmental Sciences, Wuhan University, where he is currently a Luojia Distinguished Professor. He has been supported by several talent programs, such as The Youth Talent Support Program of China (2015), China National Science Fund for Excellent Young Scholars (2014), and the New Century Excellent Talents by the Ministry of Education of China (2011). He has authored or coauthored more than 100 research papers. His research interests include image quality improvement, remote-sensing mapping and application, data fusion and assimilation, and regional and global environmental change.

Dr. Shen is currently a member of the Editorial Board of the *Journal of Applied Remote Sensing*.

Xinghua Li (S'14–M'17) received the B.S. degree in geographical information system and the Ph.D. degree in cartography and geographical information engineering from Wuhan University, Wuhan, China, in 2011 and 2016, respectively.

He is currently with the School of Remote Sensing and Information Engineering, Wuhan University, as a distinguished Associate Researcher. His current research interests focus on missing information reconstruction of remote sensing data, compressed sensing and sparse representation, image registration, image mosaicking, and remote sensing monitoring.

Dr. Li has served as a Reviewer for several journals, such as IEEE TRANSACTIONS ON GEOSCIENCE AND REMOTE SENSING, *International Journal of Remote Sensing*, IEEE JOURNAL OF SELECTED TOPICS IN APPLIED EARTH OBSERVATIONS AND REMOTE SENSING, and *Journal of Applied Remote Sensing*.

Wenxia Gan received the B.S., the M.S., and Ph.D. degrees in photogrammetry and remote sensing from Wuhan University, Wuhan, China, in 2009, 2011, 2015 respectively.

She is currently an Assistant Professor with the School of Civil Engineering and Architecture, Wuhan Institute of Technology, Wuhan, China. Her research interests include radiometric calibration and rectification of remote sensing data, application of RS/GIS on ecology environment.

Liangpei Zhang (M'06–SM'08) received the B.S. degree in physics from Hunan Normal University, Changsha, China, in 1982, the M.S. degree in optics from the Xi'an Institute of Optics and Precision Mechanics, Chinese Academy of Sciences, Xi'an, China, in 1988, and the Ph.D. degree in photogrammetry and remote sensing from Wuhan University, Wuhan, China, in 1998.

He is currently the Head of the Remote Sensing Division, State Key Laboratory of Information Engineering in Surveying, Mapping, and Remote Sensing, Wuhan University. He is also a "Chang-Jiang Scholar" Chair Professor appointed by the Ministry of Education of China. He is currently a Principal Scientist for the China state key basic research project (2011–2016) appointed by the Ministry of National Science and Technology of China to lead the remote sensing program in China. He has more than 450 research papers and 5 books. He is the holder of 15 patents. His research interests include hyperspectral remote sensing, high-resolution remote sensing, image processing, and artificial intelligence.